08.75.10

Annals of Nuclear Energy, Vol. 2, pp. 483 to 494. Pergamon Press 1975. Printed in Northern Ireland

1975

NEUTRON WAVE PROPAGATION IN MULTIPLYING ASSEMBLIES WITH AND WITHOUT CONTROL RODS

F. C. DIFILIPPO*
Departamento de Reactores, Comisión Nacional de Energía Atómica, CNEA, Buenos Aires, Argentina

(*Received* 21 *February* 1974; *in revised form* 9 *December* 1974)

Abstract—In this work the dispersion law is expanded in a power series of the frequency up to the third order; for this two group diffusion theory is used. In this manner the nuclear parameters of this approximation can be related with the experimental observables in a closed and definite form. Also a model is developed that predicts the existance of an asymptotic progagation mode even in the presence of control rods; this model permits one to calculate the wave front and the dispersion law. The models are compared with experiments done in a highly compact system with 90% ^{235}U enriched uranium fuel and H_2O moderator.

I. INTRODUCTION

The neutron wave propagation technique has advanced considerably in the last years, and is proving to be an excellent tool to study multiplying and moderating assemblies. (Perez and Uhrig, 1967; Golay, 1969; Quddus *et al.*, 1969; Wagner, 1970; Shani, 1970; Doshi and Miley, 1970; Ritchie and Whittlestone 1973).

If the assembly is excited with a neutron source of the type:

$$S = S_0 + S_1 e^{jwt}$$

at one of its faces, it can be demonstrated that the flux admits damped wave-type solutions:

$$\phi = \phi_0 + \phi_1(xy)e^{-\alpha z}e^{j(wt - \xi z)}$$

where z is the propagating direction.

In general it can be shown (MICHAEL and MOORE, 1968) that:

$$\rho^2 \equiv (\alpha + j\xi)^2 = \alpha^2 - \xi^2 + 2\alpha\xi j$$

admits a power series expansion:

$$\alpha^2 - \xi^2 = m_0 + m_2 w^2 + \dots$$

$$2\alpha\xi = m_1 w - m_3 w^3 + \dots$$

where the m_i depend on the nuclear constants, the dimensions and the shape of the assembly.

An excellent reference to the previous work in this field can be found in the paper of Perez and Uhrig (1967); the advantages of this technique and its relation to other techniques can be seen in the work of Michael And Moore.

* Present address: Neutron Physics Division. Oak Ridge National Laboratory. P. O. Box X, Oak Ridge, Tennessee 37830, U.S.A.

In the present work the m_i are related to the nuclear parameters in a closed form, so that we can determine these as a function of experimental data alone. For this analysis two group diffusion theory is used. In this way the resuls of Wagner (1970) are generalised.

The propagation of waves or pulses in heterogenous multiplying assemblies was studied by Quddus *et al.* (1969)) and by Corno (1965); in both cases the heterogeneity consited of fuel rods in a moderator.

In the present work the neutron wave propagation problem is discussed in a bare multiplying assembly in which the heterogeneity comprised control rods; for this two group diffusion theory is used. It is demonstrated that there is still an asymptotic propagation mode with the wave front distorted by the presence of the control rods; these results are extenced to the multigroup diffusion theory formalism.

The models are used to interpret experiments done in a highly compact subcritical assembly, with 90% ^{235}U enriched uranium as fuel.

II. THEORY

(a). *Neutron Wave Propagation in a Bare Subcritical Assembly Without Control Rods*

(a.1). *Two-group diffusion theory.* For an assembly defined by an infinite prism with propagation along the z axis, solutions are proposed of the form:

$$\phi_1 = \Gamma_1 \phi_\perp(xy)e^{-\rho z}e^{jwt} \quad (1)$$

$$\phi_2 = \Gamma_2 \phi_\perp(xy)e^{-\rho z}e^{jwt} \quad (2)$$

for the fast and thermal fluxes, respectively; Γ_1 and Γ_2 are the respective amplitudes and $\phi_\perp(xy)$ is the transverse flux distribution.

If w is large with respect to the precursor decay constants, the neutron balance equations give the following equation for ρ:

$$\left[\tau(B_1^2 - \rho^2) + 1 - j\frac{wl_1}{1 + k_1(1 - \beta_{ef})}\right] \times [L^2(B_2^2 - \rho^2) + 1 + jwl_2] - K = 0 \quad (3)$$

where B_1^2 and B_2^2 are, respectively, the transverse fast and thermal bucklings and the other terms are:

$$\left.\begin{aligned} k_1 &= \frac{\nu\Sigma f_1}{\Sigma r}; \quad \tau = \frac{D_1}{\Sigma r[1 - k_1(1 - \beta_{ef})]}; \\ l_1 &= \frac{1}{v_1 \Sigma r} \\ L^2 &= \frac{D_2}{\Sigma a_2}; \quad l_2 = \frac{1}{\Sigma a_2 v_2}; \\ K &= \frac{(k_\infty - k_1)(1 - \beta_{ef})}{1 - k_1(1 - \beta_{ef})} \\ k_\infty &= \frac{\nu\Sigma f_2}{\Sigma a_2}\frac{\Sigma t}{\Sigma r} + \frac{\nu\Sigma f_1}{\Sigma r} \end{aligned}\right\} \quad (4)$$

Σr is the fast removal cross section and Σt is the removal cross section of neutrons from the fast group to the thermal group. The other symbols have the usual meaning.

With the followings definitions:

$$\Delta B^2 = B_2^2 - B_1^2 \quad (5)$$

$$f = \frac{l_1}{l_2}\frac{1}{[1 - k_1(1 - \beta_{ef})]} \quad (6)$$

equation (3) takes the form (B^2 means B_2^2):

$$[\tau(B^2 - \Delta B^2 - \rho^2) + 1 + j\,wl_2 f] \times [L^2(B^2 - \rho^2) + 1 + jwl_2] - K = 0. \quad (7)$$

If we solve equation (7) for ρ^2 and we make a power series expansion in w, there results (up to the third order) the following:

$$m_0 = B^2 - \frac{1}{2}\left[\Delta B^2 - \left(\frac{1}{L^2} + \frac{1}{\tau}\right) + \sqrt{\left(\frac{1}{L^2} - \frac{1}{\tau}\right)^2 + \Delta B^2\left(\frac{2}{L^2} + \Delta B^2 - \frac{2}{\tau}\right) + \frac{4K}{L^2\tau}}\right] \quad (8)$$

$$m_1 = \frac{l_2}{L^2}\,\frac{B^2 - m_0 + \frac{1}{\tau} - \Delta B^2 + \frac{f}{\tau}[L^2(B^2 - m_0) + 1]}{2(B^2 - m_0) + \frac{1}{L^2} + \frac{1}{\tau} - \Delta B^2} \quad (9)$$

$$m_2 = \frac{\frac{l_2 m_1}{L^2} - m_1^2 + \frac{fl_2}{\tau}\left(\frac{l_2}{L^2} - m_1\right)}{2(B^2 - m_0) + \frac{1}{L^2} + \frac{1}{\tau} - \Delta B^2} \quad (10)$$

$$m_3 = \frac{m_2\left[-2m_1 + \frac{l_2}{L^2}\left(1 + \frac{L^2}{\tau}f\right)\right]}{2(B^2 - m_0) + \frac{1}{L^2} + \frac{1}{\tau} - \Delta B^2}. \quad (11)$$

If we invert equations (9), (10) and (11):

$$\frac{1}{v_2 D_2} = m_1\left[1 - \frac{1}{\frac{m_1 m_3}{m_2^2} - 1}\right] + \epsilon_1 \quad (12)$$

$$\frac{1}{\tau} = m_0 - B^2 + \Delta B^2 - \frac{m_1^3}{m_2} v_2 D_2 + \frac{m_1^2}{m_2} + \epsilon_2 \quad (13)$$

$$\frac{1}{L^2} = m_0 - B^2 - 2\frac{m_1^2}{m_2} + \frac{m_1}{m_2}\frac{1}{v_2 D_2} + \frac{m_1^3}{m_2} v_2 D_2 + \epsilon_3 \quad (14)$$

where the ϵ_i take into acount the influence of the f constant (eq. (6)). The values are:

$$\epsilon_1 = \frac{\frac{fL^2}{v_2 D_2 \tau}\left[1 + \frac{m_3}{m_2^2 v_2 D_2} - \frac{m_1 m_3}{m_2^2}\right]}{\frac{m_1 m_3}{m_2^2} - 1} \quad (12a)$$

$$\epsilon_2 = f\frac{L^2}{\tau}\left[\frac{m_1^2}{m_2} - \frac{m_1}{v_2 D_2 m_2} + m_0 - B^2 - \frac{1}{L^2}\right] \quad (13a)$$

$$\epsilon_3 = f\frac{L^2}{\tau}\left[\frac{2m_1}{v_2 D_2 m_2} + B^2 + \frac{1}{L^2} - \frac{m_1^2}{m_2} - m_0 - \frac{1}{(v_2 D_2)^2 m_2}\right]. \quad (14a)$$

If we measure m_i, B^2 and we make an estimation of ΔB^2 and f, we can determine the nuclear constants by an iterative scheme: a first guess is made by mean of equations (12), (13) and (14) ignoring the ϵ_i; with these values we estimate the ϵ_i according to eqs. (12a), (13a) and (14a), then we return to eqs. (12), (13) and (14) and so on. Finally with equation 8 we can determine K. Since $f \ll 1$ its influence on the nuclear constants is low enough and a crude approximation for this value is adequate.

(a.2). *Multigroup diffusion theory.* For the flux in the lth group, solutions are proposed of the form:

$$\phi_l = \Gamma_l \phi_{\perp}(xy) e^{-\rho z} e^{jwt} \tag{15}$$

Then, the neutron balance equation takes the form:

$$\Gamma_i \left[(1 - \beta_{ef}) \frac{\chi_i \nu \Sigma f_i}{D_i} - B_i^2 - \frac{\Sigma r_i}{D_i} - \frac{jw}{v_i D_i} \right] + \int_{l \neq i} \frac{1}{D_i} [\Sigma t_{l \to i} + (1 - \beta_{ef}) \chi_i \nu \Sigma f_l] \Gamma_l = -\rho^2 \Gamma_i \tag{16}$$

where χ_i, B_i^2 and Σr_i are, respectively, the fission spectrum, the transverse buckling and the removal cross section in the group i; $\int$ means summation over indices and the other symbols have their usual meaning. In order to solve the $n \times n$ system (eq. (16)) (n number of energy group), we must diagonalize a matrix whose terms are:

$$A_{il} = \frac{1}{D_i} [\Sigma t_{l \to i} + (1 - \beta_{ef}) \chi_i \nu \Sigma f_l] \quad i \neq l \tag{17}$$

$$A_{ii} = (1 - \beta_{ef}) \frac{\chi_i \nu \Sigma f_i}{D_i} - B_i^2 - \frac{\Sigma r_i}{D_i} - \frac{jw}{v_i D_i} \tag{18}$$

The eigenvalue of this matrix is $-\rho^2$.

(b). *Neutron Wave Propagation in a bare Subcritical Assembly With Control Rods*

(b.1). *Two group diffusion theory.* Figure 1 represents the section normal to the propagation direction (z); the assembly is an infinite prism of transverse section a, b and there are absorbing plates parallel to the plane $y = 0$ placed in a symmetrical manner with respect to the xy axes. The plane source, placed at $z = 0$, is also symmetrical with respect to these axes.

In control rod theory there is defined (Maynard, 1964):

$$\kappa = \frac{J_A - J_B}{\phi_A + \phi_B} \tag{19}$$

where J_A, ϕ_A, J_B, ϕ_B are, respectively, the current and the flux at each side of the absorbing plate.

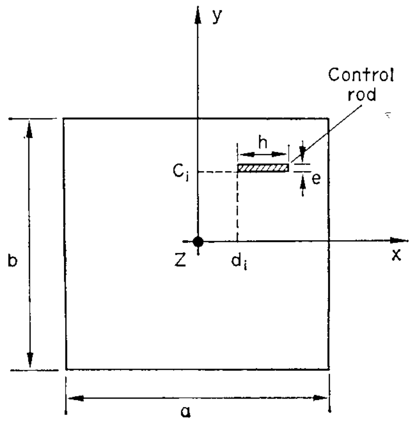

Fig. 1. Cross section of the system with control rods; z is the propagation direction.

The absorption in the plate per unit area is:

$$\delta a = J_A - J_B = \kappa(\phi_A + \phi_B) = 2\kappa\phi \tag{20}$$

where ϕ is the average flux in the plate.

If the thickness e is small, the spatial distribution (δA) of the plate absorption, is, per unit volume:

$$\delta A = \sum_{i=1}^{M} \phi(xyz) 2\kappa\, \delta(y - c_i) \times [H(x - d_i) - H(x - d_i - h)] \tag{21}$$

where M is the number of plates, δ is the Dirac delta function and H is the step function.

If we consider that the plates only absorb thermal neutrons, the balance equations in two group diffusion theory are:

$$D_1 \nabla_{xy}^2 \phi_1 + D_1 \frac{\partial^2 \phi_1}{\partial z^2} - \Sigma r \phi_1 + \nu \Sigma f_1 (1 - \beta_{ef}) \phi_1 + \nu \Sigma f_2 (1 - \beta_{ef}) \phi_2 = \frac{1}{v_1} \frac{\partial \phi_1}{\partial t} \tag{22}$$

$$D_2 \nabla_{xy}^2 \phi_2 + D_2 \frac{\partial^2 \phi_2}{\partial z^2} - \Sigma a \phi_2 + \Sigma t \phi_1 - \delta A + S(xy)\, \delta(z) e^{jwt} = \frac{1}{v_2} \frac{\partial \phi_2}{\partial t} \tag{23}$$

in which S is the amplitude of the source placed at $z = 0$.

We will expand the fluxes and the source according to:

$$\phi_1 = \sum_{mm} E_{nm}(z)\psi_{mm}(xy)e^{jwt} \quad (24)$$

$$\phi_2 = \sum_{nm} F_{nm}(z)\psi_{nm}(xy)e^{jwt} \quad (25)$$

$$S(xy) = \sum_{nm} S_{nm}\psi_{nm}(xy) \quad (26)$$

As a consequence of the xy symmetry, the ψ_{nm} satisfy:

$$\nabla_{xy}^2\psi_{nm} = -B_{nm}^2\psi_{nm} \quad (27)$$

$$\psi_{nm} = \frac{2}{\sqrt{ab}}\cos(2n+1)\frac{\pi}{a}x \times \cos(2m+1)\frac{\pi}{b}y \quad (28)$$

$$\langle\psi_{nm}, \psi_{kl}\rangle = \delta_{nk}\,\delta_{ml}; \qquad n, m = 0, 1, 2, 3, \ldots \quad (29)$$

where B_{nm}^2 is the tranverse buckling of the nm mode, δ_{nk} the Kroenecker delta and the brackets denote scalar product.

If we sustitute ϕ_1, ϕ_2 and S, according to equations (24), (25) and (26), in eqs (22) and (23) and after that we multiply scalarly by ψ_{hp}, we obtain:

$$D_1\frac{d^2E_{hp}}{dz^2} - a_{hp}E_{hp} = -\nu\Sigma f_2(1-\beta_{ef})F_{hp} \quad (30)$$

$$D_2\frac{d^2F_{hp}}{dz^2} - b_{hp}F_{hp} = -S_{hp}\,\delta(z) - \Sigma tE_{hp} + 2\kappa\sum_{(nm)\neq(hp)} C_{\substack{nm\\hp}}F_{nm} \quad (31)$$

where:

$$a_{hp} = \Sigma r - \nu\Sigma f_1(1-\beta_{ef}) + D_1B_{hp}^2 + \frac{jw}{v_1} \quad (32)$$

$$b_{hp} = \Sigma a + D_2B_{hp}^2 + j\frac{w}{v_2} + 2\kappa C_{\substack{hp\\hp}} \quad (33)$$

$$C_{\substack{nm\\hp}} = \sum_{i=1}^{M} C^i_{\substack{nm\\hp}} \quad (34)$$

$$C^i_{\substack{nm\\hp}} = \frac{4}{ab}\left[\cos(2m+1)\frac{\pi}{b}c_i\cos(2p+1)\frac{\pi}{b}c_i\right] \times \int_{di}^{di+h}\cos(2n+1)\frac{\pi}{a}x\cos(2h+1)\frac{\pi}{a}x\,dx \quad (35)$$

$(nm) \neq (hp)$ means that $n \neq h$ and/or $m \neq p$.

If we make the spatial Fourier transform (s is the transformed variable) of equations (30) and (31), we obtain for the transform of F_{hp} ($\bar{F}_{hp}$):

$$\bar{F}_{hp}(s) = -\frac{S_{hp}(D_1s^2 + a_{hp})}{\sqrt{2\pi}\,[\Sigma t\nu\Sigma f_2(1-\beta_{ef}) - (D_2s^2 + b_{hp})(D_1s^2 + a_{hp})]} + \frac{2\kappa(D_1s^2 + a_{hp})}{[\Sigma tJ\Sigma f_2(1-\beta_{ef}) - (D_2s^2 + b_{hp})(D_1s^2 + a_{hp})]} \times \sum_{(nm)\neq(hp)} C_{\substack{nm\\hp}}\bar{F}_{nm} \quad (36)$$

Equation (36) tells us that the hp mode appears even in the case in which it is not excited by the source ($S_{hp} = 0$); the parameter $C_{\substack{nm\\hp}}$ "tranforms" the mode nm into an hp mode and depends on the position of the plates.

If we perform the inverse transform of equation (36), we obtain:

$$F_{hp}(z) = -\frac{S_{hp}}{\sqrt{2\pi}}[A_{hp}e^{-\rho_{1hp}|z|} + B_{hp}e^{-\rho_{2hp}|z|}] + \frac{2\kappa}{\sqrt{2\pi}}[A_{hp}e^{-\rho_{1hp}|z|} + B_{hp}e^{-\rho_{2hp}|z|}] * \sum_{(nm)\neq(hp)} C_{\substack{nm\\hp}}F_{nm}(z) \quad (37)$$

where $*$ indicates convolution and ρ_{1hp}, ρ_{2hp} are solutions of:

$$\rho^4 - \left(\frac{b_{hp}}{D_2} + \frac{a_{hp}}{D_1}\right)\rho^2 + \frac{b_{hp}a_{hp} - \Sigma t\nu\Sigma f_2(1-\beta_{ef})}{D_1D_2} = 0 \quad (38)$$

In equation (37) only the damping wave solutions appear; the subindex 1 indicates the asymptotic solution for ρ, and we have for the A_{hp} and B_{hp}:

$$A_{hp} = \sqrt{\frac{\pi}{2}}\frac{1}{\rho_{1hp}}\frac{a_{hp} - D_1\rho^2_{1hp}}{D_1D_2(\rho^2_{1hp} - \rho^2_{2hp})} \quad (39)$$

$$B_{hp} = \sqrt{\frac{\pi}{2}}\frac{1}{\rho_{2hp}}\frac{D_1\rho^2_{2hp} - a_{hp}}{D_1D_2(\rho^2_{1hp} - \rho^2_{2hp})} \quad (40)$$

We can solve equation (37) by successive approximation; the zero approximation will be:

$$F_{nm}(z) = -\frac{S_{nm}}{\sqrt{2\pi}} \times [A_{nm}e^{-\rho_{1nm}|z|} + B_{nm}e^{-\rho_{2nm}|z|}] \quad (41)$$

and in the first order, substituting equation (41) into (37)

$$F_{hp}(z) = -\frac{S_{hp}}{\sqrt{2\pi}}[A_{hp}e^{-\rho_{1hp}|z|} + B_{hp}e^{-\rho_{2hp}|z|}]$$

$$-\frac{\kappa}{\pi}\sum_{(nm)\neq(hp)} C_{\substack{nm\\hp}} S_{nm}$$

$$\times [A_{hp}e^{-\rho_{1hp}|z|} + B_{hp}e^{-\rho_{2hp}|z|}]$$

$$* [A_{nm}e^{-\rho_{1nm}|z|} + B_{nm}e^{-\rho_{2nm}|z|}] \qquad (42)$$

If we make the convolution in equation (42) and substitute the result in equation (25), we obtain for the asymptotic solution (those terms in which appears exp $(-\rho_{100}z)$)

$$\phi_2(xyzt) = e^{-\rho_{100}z}F(xyw)e^{jwt} \qquad z > 0 \qquad (43)$$

where:

$$F(xyw) = \frac{-S_{00}A_{00}\psi_{00}}{\sqrt{2\pi}} + \frac{2\kappa}{\pi}\sum_{(nm)\neq(00)}$$

$$\times\left\{\frac{A_{nm}\rho_{1nm}}{\rho_{100}^2 - \rho_{1nm}^2} + \frac{B_{nm}\rho_{2nm}}{\rho_{100}^2 - \rho_{2nm}^2}\right\}$$

$$\times A_{00}\cdot C_{\substack{00\\nm}}(S_{00}\psi_{nm} + S_{nm}\psi_{00}) \qquad (44)$$

Equation (43) tells us that there is still an asymptotic wave whose wave front is given by eq (44); this is distorted by the presence of the rods. According to the model, ρ_{100} is calculated with the same cross sections of the system without control rods, but Σ_a' is affected by the additional absorption of the rod:

$$\Sigma a' = \Sigma a + 2\kappa C_{\substack{00\\00}} \qquad (45)$$

in which Σ_a is the thermal absorption cross section of the system without control rods.

(b.2). *Multigroup diffusion theory.* In order to calculate the dispersion law of the system with control rods the result obtained in the last section can be extended to a multigroup formalism; the balance equations are in this case:

$$D_k\nabla_{xy}^2\phi_k + D_k\frac{\partial^2\phi_k}{\partial z^2} - \Sigma r_k\phi_k + \int_{l\neq k}\Sigma t_{l\to k}\phi_l$$

$$+ (1-\beta_{ef})\chi_k\int_l \nu\Sigma f_l\phi_l - \delta A^k = \frac{1}{v_k}\frac{\partial\phi_k}{\partial t} \qquad (46)$$

δA^k is the same as in equation (21) but now κ is a function of the group index k. If we put into eq. (46) solutions of the form:

$$\phi_k = e^{jwt}e^{-\rho z}f_k(xyw) \qquad (47)$$

with

$$f_k = \sum_{nm} F_{nm}{}^k\psi_{nm}(xy) \qquad (48)$$

where the ψ_{nm} are defined in equations (27–29), and after that we multiply scalarly by ψ_{hp}, we obtain:

$$F_{hp}{}^k\Big[-D_kB_{hpk}^2 + \rho^2D_k - \Sigma r_k$$

$$+ \chi_k(1-\beta_{ef})\nu\Sigma f_k - j\frac{w}{v_k} - 2\kappa_kC_{\substack{hp\\hp}}\Big]$$

$$+\int_{l\neq k}[\Sigma t_{l\to k} + \chi_k(1-\beta_{ef})\nu\Sigma f_l]F_{hp}{}^l$$

$$= \sum_{(nm)\neq(hp)} 2F_{nm}{}^k\kappa_kC_{\substack{nm\\hp}} \qquad (49)$$

where B_{hpk}^2 is the buckling of the hp mode corresponding to the group k and the $C_{\substack{nm\\hp}}$ are defined in equations (34) and (35). In order to solve equations (49) we can use successive approximation; the zero order approximation corresponds to the case without control rods, in this case:

$$F_{nm}{}^k = \Gamma^k\,\delta_{n0}\,\delta_{m0} \qquad (50)$$

because we are assuming to be far from the source. Then we obtain for the first coefficient in equation (48), in the first order approximation:

$$F_{00}{}^k\Big[-D_kB_{00k}^2 + \rho^2D_k - \Sigma r_k$$

$$+ \chi_k(1-\beta_{ef})\nu\Sigma f_k - j\frac{w}{v_k} - 2\kappa_kC_{\substack{00\\00}}\Big]$$

$$+\int_{l\neq k}[\Sigma t_{l\to k} + \chi_k(1-\beta_{ef})\nu\Sigma f_l]F_{00}{}^l = 0 \qquad (51)$$

which has the same form as equation (16).

Then ρ is calculated in the same manner as in the system without control rods but with the removal cross section of the group k affected by an additional term:

$$\Sigma r_k' = \Sigma r_k + 2\kappa_kC_{\substack{00\\00}} \qquad (52)$$

III. EXPERIMENTAL ARRANGEMENT

A scheme of the system to be measured and the block diagram of the measurement equipment can be seen in Fig. 2. The subcritical assembly is compound of 16 MTR fuel element in a 4×4 configuration. Each element has the dimensions: $8{\cdot}04\times7{\cdot}62\times75{\cdot}5\ \mathrm{cm}^3$ and contains 19 aluminim-clad, 90% ^{235}U enriched uranium fuel plates. An Al tank of 3 mm wall thickness contains the fuel elements; between the tank and the multiplicative assembly there is an 0·8 mm Cd sheet.

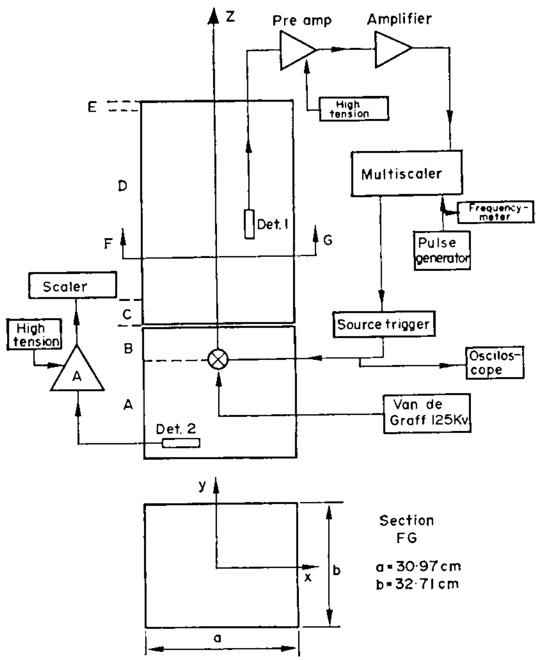

Fig. 2. Diagram of the experimental set-up.

The moderator, H_2O, fills the fuel elements; the dimensions, indicated in Fig. 2, are taken between "black" surfaces (i.e. the Cd surfaces).

The pulsed neutron source, of the SAMES type with the PHILLIPS neutron generator, produces 14 Mev neutron through the D–T reaction. It is in a water tank below the multiplicative assembly in order to shield the source neutrons. The system has a $K_{ef} = 0{\cdot}774$, calculated with four group diffusion theory, using the code EXTERMINATOR II (Fowler et. al. 1967) and with the necessary cross sections (Solanilla *et al.*, 1971).

From bottom to top we have the following regions: A, 30 cm of water; B, 8 cm of water; C, 7 cm of a water–aluminium mixture; D, multiplicative region of 61·5 cm height composed of H_2O, Al, ^{235}U and ^{238}U; E, 2 cm of a water–aluminium mixture. The tritium target is placed at $x = y = 0$; in this manner only even harmonics are excited in the xy plane.

The detector system which begins with the detector 1 is used to measure the pulse response as a function of z. It is composed of : Reuter–Stokes ^3He detector model SK-585 with 6 mm dia and an active length of 5 cm, ORTEC preamplifier mod 109 PC, ORTEC amplifier mod 410, multichannel analyser TMC with the 212 plug in unit.

The detector system which begins with the detector 2 is used to normalize the measured neutron distribution. It is composed of: 20th Century BF_3 detector (enriched in ^{10}B) of 1·3 cm dia and 5 cm active length mod 5 EB40/13, charge amplifier and scaler developed in CNEA. The dead times of both systems are respectively 1·2 and 7 μsec. In order to introduce the detector a normal fuel plate was removed and a special one was introduced.

The system described above, was measured without and with Cd plates; in this case there were introduced two plates of 4 cm width, 0·8 mm thick, along the z axes, in the $y = 0$ plane, in the coordinate $x = \pm 6$ mm (d_i) (See Fig. 1).

IV. EXPERIMENTAL PROCEDURE

In order to see propagation effects it is necessary that the measured zone be free of source neutrons; a common method is to thermalize the 14 Mev neutrons and then to measure the Cd difference. This was intended in the system described in Fig. 2; for this, the source was located in the lower tank at a distance of 30 cm from the beginning of the fuel element. Owing to an access problem the Cd shutter could be put at 7 cm from the beginning of the fuel; this 7 cm (part C in Fig. 2) is compounded of water and the aluminium of the structural part of the fuel element. Thus the thermal neutrons have very low probability of crossing this zone, so that the Cd difference was unsuccessful.

Taking into account this situation, we adopted the solution proposed by Golay (1969): The first collision source is estimated and if it is demonstrated that this source is concentrated in a region outside of the measured zone, it is possible to do the measurement without the Cd difference. In this, the basic idea is that the source neutrons becomes thermal not too far from the point in which they make their first collisions. This hypothesis is reasonable because our systems are moderated by hydrogen and the neutrons after their first collision can loose their energy or degrade it in such a way that the mean free path between collision is considerably diminished. The total cross section of the 14 MeV neutrons in water is large enough to assure, in our case, that 95% of the source neutrons that interact with the multiplicative assembly make their first collision below the first experimental point taken into account in measuring the dispersion law.

To measure the pulse response as a function of z, we put the detect or in the coordinate $x = a/6$ $y = b/6$, i.e. it is insensitive to the 01, 10, 11 modes. The systems were excited with neutrons pulses of 50 μsec width and a repetition rate of $\sim$308 p.p.s.;

in all the cases the channel width was 10 μsec. The source was operated for 3 min without analyzing in order to obtain the delayed neutron equilibrium response. When the constant delayed neutron density was achived, the detector system was operated until the desired counting statistics were obtained. The source and detector systems were then simultaneously shut off. The statistics in the peaks ranges from ~10,000 counts for the points near the source to ~3000 counts for the farthest, the measuring times go from 10 min to 50 min, respectively.

Dead time effects can be corrected in the detector 1 system but it is not possible in the normalization detector system. This is due to the fact that the latter integrates in time. The counts lost in this case were estimated, and it was demonstrated to be below 3‰. For this evaluation it was assumed that the count rate had exponential plus background behavior.

V. CALCULATIONAL PROCEDURE

(a). *Data Processing*

After correcting for the dead time effect and background, our experimental data are the prompt neutron response in channel i(the corresponding time is t_i) measured with the detector in position z, $n(t_i, z)$.

The frequency response of the system is given by the Fourier transform of counting rate $c(t, z)$:

$$F(w, z) = \int_0^\infty c(t, z)e^{jwt}\, dt \tag{53}$$

This integral can be divided into three parts; the first between zero and t_1, the second between t_1 and t_2 and the third between t_2 and ∞. The TMC multichannel analyzer has a waiting time before beginning the time analysis. Thus between $t = 0$ and $t = t_1$ we have no information; for times greater than t_2, the prompt response is masked by the delayed response. In our case t_2 was selected in such a way that for this time the number of count is twice the background level. Then the integral of equation (53) can be done numerically between t_1 and t_2. Between zero and t_1 it is necessary to interpolate and between t_2 and ∞ is necessary to extrapolate.

To extrapolate and to interpolate, the last and the first channels were fitted according to:

$$n(t, z) = Ae^{-\lambda t} \tag{54}$$

$$n(t, z) = A(1 - e^{-\beta t})e^{-\lambda t} \tag{55}$$

respectively.

Table 1. Influence of the non-measurable part of the equilibrium pulse, over the Fourier transform. Typical values

	Frequency (Hz)	(a) (%)	(b) (%)
Amplitude	200	−1·7	−0·089
	1000	−0·8	−0·44
Phase	200	1·7	−1·5
	1000	2·3	−0·35

(a) Error when the interpolation is not included.
(b) Error when the extrapolation is not included.

With equations (54) and (55) the contributions of the non-measurable zones of the response pulse in equation (53) were calculated. These contributions can be estimated as in Table 1: we can observe the contributions are small enough so that the possible inaccuracy of equations (54) and (55) can be neglected.

A FORTRAN IV code FOURIER was written in order to calculate the integral in equation (53). The input of the code is the Multichannel analyzer data and the number of counts in the normalization detector. After the calculations, the normalized amplitude and the phase of the Fourier transform with the corresponding errors are punched on cards.

Now the amplitude $|F(w, z)|$ and phase $\varphi(w, z)$ must be analyzed as a function of z for each frequency in order to obtain the dispersion law.

Let ϕ_w be the complex amplitude of the wave at frequency w, and impose the boundary condition:

$$\phi_w(Z = L) = 0 \tag{56}$$

Then we will have a reflected wave toward the negative values of z:

$$\phi_w = Ae^{-\alpha z}e^{j(\eta - \xi z)} + Be^{\alpha z}e^{j\xi z} \tag{57}$$

Where A is real. Then according to eq. (56):

$$\phi_w = Ae^{-\alpha z}e^{-j(\xi z - \eta)}[1 - e^{-2\alpha(L-z)}e^{-2j\xi(L-z)}] \tag{58}$$

which means that:

$$\frac{\phi_w}{k}e^{-j\delta} = Ae^{-\alpha z}e^{-j(\xi z - \eta)} \tag{59}$$

where:

$$k = \sqrt{[1 - e^{-2\alpha(L-z)}\cos 2\xi(L - z)]^2 + e^{-4\alpha(L-z)}\sin^2 2\xi(L - z)} \tag{60}$$

$$\delta = \operatorname{arctg}\frac{e^{-2\alpha(L-z)}\sin 2\xi(L - z)}{1 - e^{-2\alpha(L-z)}\cos 2\xi(L - z)} \tag{61}$$

Equation (59) suggests an iterative method; given the experimental data ϕ_w, we fit them for a first estimation of α and ξ according to the right member of equation (59). With these values we calculate k and δ which permit one to correct ϕ_w and so forth.

For these calculations, a FORTRAN IV code RELDI was developed; with the input data provided by Fourier, it calculates α and ξ by the iterative method proposed, the m_i of the $\alpha^2 - \xi^2$ and $2\alpha\xi$ expansions and the corresponding errors.

(b). *Numerical Calculations of the Models*

For this purpose several codes were developed; the FORTRAN IV code ON2G calculates the dispertion law in two-group diffusion theory. It also calculates the influence of the cross sections on α and ξ; for this, systematic variations of cross sections are made. The FORTRAN IV code ON4G calculates the dispersion law with four-group diffusion theory; for this, the code uses the complex subroutines POLCAR and RAICES (Grant, 1971) which permits one to diagonalize a $n \times n$ complex matrix with an arbitrary n.

Finally the code ONDAS calculates ϕ (x, y, z, w) according to equation (43); also it calculates the spatial transients before arriving at the asymptotic solution (i.e. equation 43)

VI. RESULTS AND INTERPRETATION

After the measurements of the equilibrium pulses as a function of z, the experimental data were processed by the Fourier code; part of the results are shown in Figs. 3 and 4. In these we can see the amplitude $|F(w, z)|$ and the phase φ (w, z) of the measured Fourier transform as well as the values corrected by end effect. In the case where the two values coincide within the scale, only the former is presented; also the results of the fit between $z = 40$ cm and $z = 64$ cm (distance with respect the source position) are represented.

Figures 3 and 4 correspond to the case with control rods. We can see that it is experimentally demonstrated that an asymptotic mode exists even in the presence of Cd plates. However, at approximately 720 Hz, the phase begins to be non-linear with respect to the detector position; the effect is more pronounced at very high frequencies. For example, at 2 kHz we can see in Fig. 4 the non-linearity even with the end effect correction. In this sense the results are similar to the case without control rods. Since the proposed asymptotic solutions are not valid for high frequencies, the results are analysed up to 720 Hz.

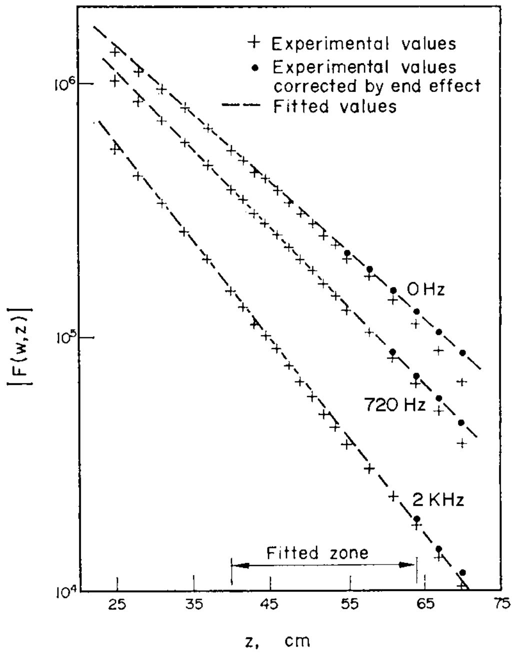

Fig. 3. Amplitude of the Fourier transform for the system with control rods. The errors are less than the values shown; z is measured from the source plane.

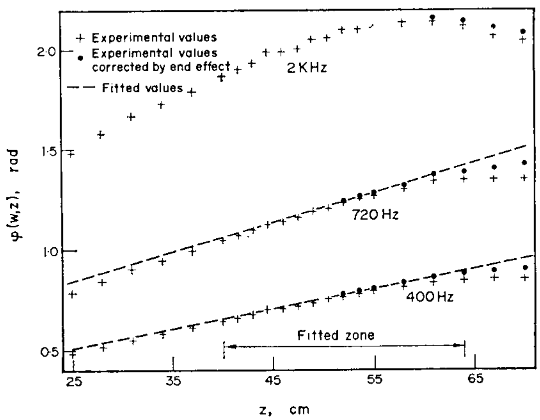

Fig. 4. Phase of the Fourier transform for the system with control rods. The errors are less than the values shown; z is measured from the source plane.

In order to analize this behavior it must taken into account that the homogeneous hypothesis is reasonable because the heterogeneity of the fine thermal flux distributions between the fuel plates is less than 5%. Then the phase behaviour as a function of detector position hardly can be explained by heterogeneity effects.

Also in Figs. 3 and 4 the importance and the accuracy of the end effect corrections can be observed; the iterative method proposed in section

Table 2. Results of the measurements of the dispersion law, up to 720 Hz

	m_0 (cm^{-2})	m_1 (cm^{-2} sec)	m_2 cm^{-2} sec^2	m_3 (cm^{-2} sec^3)
System without control rods	$(2{\cdot}90 \pm 0{\cdot}07) \times 10^{-3}$	$(7{\cdot}37 \pm 0{\cdot}36) \times 10^{-7}$	$(6{\cdot}26 \pm 0{\cdot}94) \times 10^{-11}$	$(4{\cdot}88 \pm 3{\cdot}19) \times 10^{-15}$
System with control rods	$(3{\cdot}86 \pm 0{\cdot}10) \times 10^{-3}$	$(5{\cdot}58 \pm 0{\cdot}45) \times 10^{-7}$	$(4{\cdot}78 \pm 1{\cdot}14) \times 10^{-11}$	$(4{\cdot}49 \pm 3{\cdot}80) \times 10^{-15}$

V was used to process the data between $z = 40$ cm and $z = 64$ cm; the corrections so obtained not only align the points taken in the fit but also the others as well. Ordinarily this kind of measurement is made in systems long enough to neglect experimental data near the border; the proposed method avoids this problem.

For the system without control rods, the equilibrium pulse was measured as a function of y, in $z = 47{\cdot}5$ cm and $x = 5{\cdot}16$ cm; the selected z coordinate is within the fitted zone to obtain the dispersion law. After making the Fourier transform and normalizing, the results are shown in Fig. 5; the continuous lines are the results of the fit according to Acos By. These measurements, in conjunction with results similar to those show in Figs. 3 and 4, permit one to confirm the separation of variables proposed in equation (2); furthermore, these facts demonstrate that the fitted zone is free of harmonics.

The bucking so measured in the y direction, was practically independent of the frequency; its variation between zero and 1 kHz was $-2{\cdot}4\permil$. The extrapolation distance so obtained was $(2{\cdot}26 \pm 0{\cdot}10)$ cm and the thermal transverse buckling was then 149 ± 1 m^{-2}.

After the measurement of α and ξ these values were fitted as a function of the frequency in order to obtain the m_i; the results are shown in Table 2. The value of ΔB^2 was determined by means of the Exterminator II code and the corresponding cross sections to be $19{\cdot}4$ m^{-2}. The influence of this parameter over the m_i for the systems studied was evaluated by the calculation of $(\partial m_i/\partial \Delta B^2)\,(\Delta B^2/m_i)$ according to equation (7) to (10); the results are shown in Table 2. We observe that with the exception of m_0 the m_i are quite insensitive to the value of ΔB^2.

Table 3. Influence of ΔB^2 over the m_i for the studied system

	m_0	m_1	m_2	m_3
$\dfrac{\partial m_i}{\partial \Delta B^2}\dfrac{\Delta B^2}{m_i}$	0·577	−0·0109	−0·0149	−0·0176

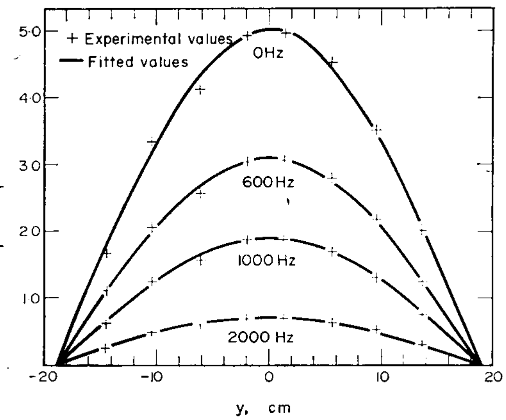

Fig. 5. Transverse flux measurement as a function of frequency for the system without control rods. The errors are less than the values shown.

If with the experimental m_i and B^2 and the calculated ΔB^2, we calculate τ according to equation (13), we obtain a negative value for this parameter even within the experimental error. The sign of this calculation is independent of the values of the others parameters that appear in equation. (13) (through ϵ_2). Thus we conclude that two group diffusion theory cannot explain our experimental results.

Two and four-group diffusion theory calculations of the dispersion law are shown in Fig. 6 together

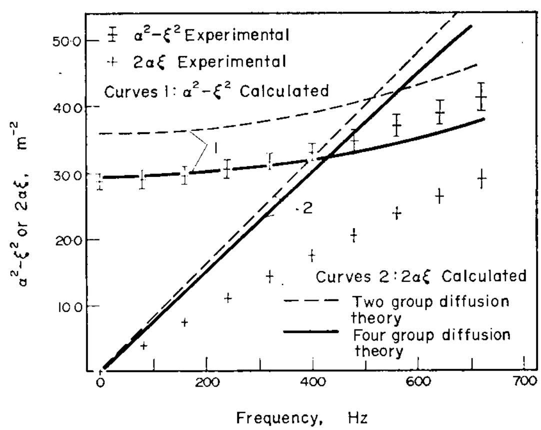

Fig. 6. $\alpha^2 - \xi^2$ and $2\alpha\xi$ for the system without contro rods; the vertical bars indicate the errors.

with the experimental results. Both approximation have the same thermal group cross sections. The fast cross sections in two-group theory are the result of the condensation of the three fast groups of the four-group approximation. The cross sections were calculated by Solanilla *et al.* (1971). The mean velocity of thermal neutrons was calculated by the Thermos code (Stammler, 1963); in the calculation of the dispersion law the experimental thermal buckling (B_{th}^2) were introduced and the $\Delta B_i^2 \equiv B_{th}^2 - B_i^2$ calculated by the Exterminator II code.

If we compare the two- and four-groups calculations with the experimental results, we conclude that increasing the number of fast groups permits a better estimation of m_0 but there still exist discrepancies between the calculated and measured m_i ($i \neq 0$). In Fig. 7 we observe the theoretical and experimental values of the dispersion law for the system with control rods. The former are calculated with four-group diffusion theory with the same cross sections of the system without control rods with the exception of the thermal absorption cross section which is affected by the additional term of equation (45). For this the value $\kappa = 0{\cdot}5$ was used (Maynard, 1964).

The wave front, as a function of y, measured and calculated according to equation (43) can be seen in Figs. 8 and 9, both values correspond to the coordinates $z = 46$ cm, $x = 2{\cdot}15$ cm; the calculations were made with two kinds of source distribution: constant and fundamental mode in x, y. The experimental values conserve the proportionality with frequency; the theoretical values are normalized for each frequency to the experimental points. Then in Figs. 8 and 9 we compare the shapes of the wave front for each frequency.

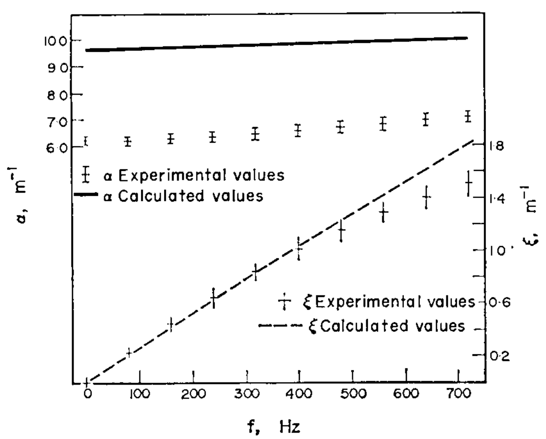

Fig. 7. α and ξ for the system with control rods; the vertical bars indicate the errors. The calculated values correspond to four-group diffusion theory.

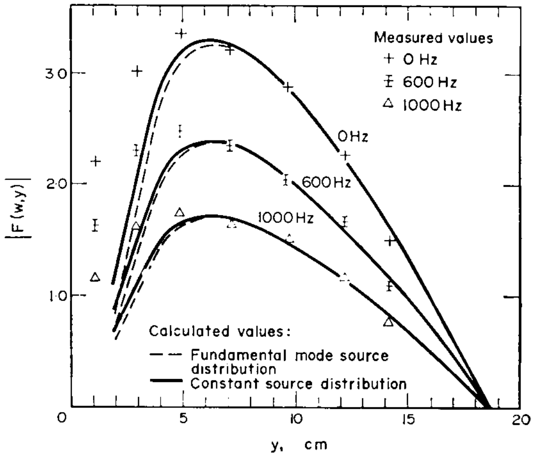

Fig. 8. Amplitude of the wave front in the system with control rods. The errors are less than the values shown.

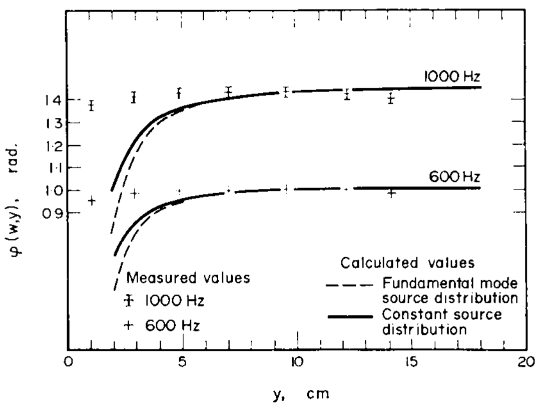

Fig. 9. Phase of the front wave in the system with control rods. The errors are less than the values shown.

We can see that for points placed at more than 5 cm from the plates the model calculates correctly the shape of the wave front. For point nearer to the plates the results depends on the source distribution. We can see in Figs. 8 and 9 that the presence of negative harmonics for the source, rise the theoretical results toward the experimental values; if we take into account that the thermal source is depressed by the presence of the control rods (and then increasing its negative harmonics contents) these results can explain the differences observed near the plates.

In Figs. 10 and 11 the frequency behavior of the wave front is analyzed, the theoretical and experimental values correspond to the relation between the amplitudes of the thermal fluxes at frequency w and frequency zero, and the phase. The values correspond to the same coordinates as before

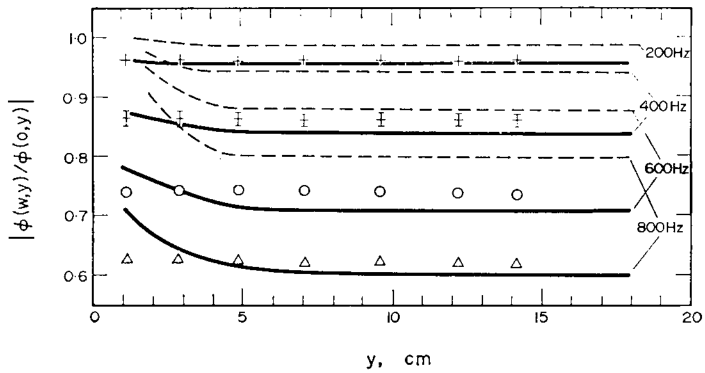

Fig. 10. Relative amplitude of the thermal flux at frequency w with respect to the zero frequency flux. Measured values: +, 200 Hz; ⫯, 400 Hz; ⊙, 600 Hz; △, 800 Hz; the symbols indicate the errors. Calculated values: ---- equation (43) with dispersion law calculated by two-group diffusion theory; ——— the former results corrected by the observed difference between the experimental and theoretical dispersion law.

The dashed lines in Figs. 10 and 11 correspond to the calculation of wave front according to equation (43) using the corresponding two-group cross sections; but as we can see in Fig. 7, the theory calculates a less dispersive system than we observed. If we take into account the difference between the experimental and theoretical dispersion law, we can correct the previous results by this effect. The results of these corrections are shown in Figs. 10 and 11 by the continuous line. Then we conclude that equation (43) describes correctly the shape, and the frequency behavior of the flux if we include in the calculations the correct dispersion law.

VII. CONCLUSION

The power frequency expansion of the dispersion law up to the third order permits one to relate in a closed and definite manner the nuclear parameters of the two-group diffusion theory; with the different terms of the expansion (the m_i), we can relate directly these constants to experimental values. In the development of these relations energy depending bucklings were included and there was demonstrated the importance of the difference between the thermal and fast bucklings in the m_0, and that this effect in the calculation of the m_i with $i \neq 0$ can be neglected.

A model was also developed that predicts the existance of an asymptotic mode of propagation even with the presence of control rods. The wave front is distorted by the presence of the control rod and the dispersion law is shifted with respect to the case without control rods. This shift depends

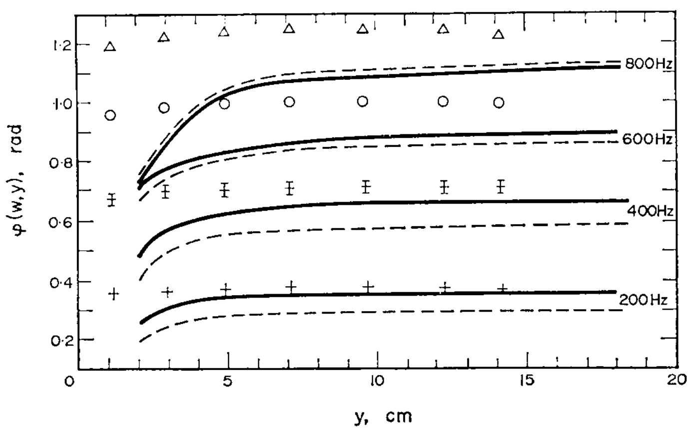

Fig. 11. Phase of the thermal flux. Measured values: +, 200 Hz; ⫯, 400 Hz; ⊙, 600 Hz; △, 800 Hz; the errors are less than the values shown. Calculated values: ---- equation (43) with the dispersion law calculated by two-group diffusion theory; ——— the former results corrected by the observed differences between the experimental and theoretical dispersion law.

of κ, the constant of the control rod theory (Maynard, 1964) and the positions of the rods.

The preceding models were used to interpret experiments made with a highly compact system of 90% ^{235}U enriched uranium with and without control rods. It was demonstrated in this case that two-group diffusion theory is incompatible with the experimental results. For the system with control rod, the experimental results confirm the existance of an asymptotic mode which was theoretically predicted.

Also the model gives a good estimation of the wave front shape and its frequency behavior, with the exception of points near the control rods. The theoretical values of the dispersion law are improved on increasing the number of energy groups in the calculations. It is noted also that the discrepancies between the experimental and calculated values of the dispersion law, are approximately the same in the systems with and without control rods. In a recent paper (Sobhana *et al.*, 1973) the necessity, of having a good description of the slowing down and thermalization effects, in order to calculate correctly the dispersion law was demonstrated. In the paper of reference multigroup diffusion theory was used with 18 thermal groups and 12 fast groups.

Acknowledgements—I am grateful to the following persons from the Departamento de Reactores, CNEA, whose efforts made this work possible: R. M. Waldman, A. Gomez and J. Vicente. I am grateful to C. Castromadero and H. M. Antunez for reading and commenting the manuscript, and I am indebted to T. F. Parkinson for his assistance in the preparation of this report.

REFERENCES

Corno S. E. (1965) Theory of pulsed neutron experiments in highly heterogeneous multiplying media. in *Pulsed Neutron Research*, Vol. I, *Proceeding of a Symposium*, Karlsruhe 1965. IAEA Vienna (1970).

Doshi P. K. and Miley G. H. (1970) Neutron pulse propagation in a multiple medium. *Nucl. Sci. Engng* **39**, 182.

Fowler T. B., Tobias M. L. and Vondyd R. (1969). EXTERMINATOR II a FORTRAN IV code for solving multigroup diffusion equations in two dimension, ORNL-4078 (1967).

Golay M. W. Neutron pulse propagation in multiplying assemblies. Ph.D. Thesis, Cornell University, Ithaca, New York.

Grant C. (1971) Private comunication.

Maynard C. W. (1964) Naval Reactor Physics Handbook, Vol I, Page 409, USAEC.

Michael P. and Moore M. N., Relation between pulsed, poisoning and wave experiments. In: *Neutron Thermalization and Reactor Spectra, Proceedings of a Symposium*, Ann Arbor, July 1967. IAEA Vienna 1968, Vol I.

Perez R. B. and Uhrig R. E. (1967) "Development of techniques of neutron wave and pulse propagation in Neutron noise, waves and pulse propagation. AEC 9 Symposium series,

Quddus M. A., Cochran R. G. and Emon D. E. (1969) Axial propagation of neutron waves in heterogenous media. *Nucl. Sci. Engng*. **35**, 342.

Ritchie A. I. M. and Whittlestone S. (1973) Measurement of thermal neutron waves at high frequencies in Be O. *J. nucl. Energy* **27**, 335.

Shani G. (1970) Neutron waves in reflected reactors. Ph.D. Thesis, Cornell Univ., Ithaca, N. Y.

Sobhana S., Goyal I. C., Singh OM Ral and Gnatak A. K. (1973) Study of neutron wave propagation through a subcritical assembly, *J. Nucl. Energy* **27**, 441.

Solanilla R., Pasquini E., Pieroni N., Rapoport H. and Ricabarra H. (1971) "Correlación experiencia teoria en el reactor RA 3 CNEA 303.

Stmm' Ler R. J. J. (1963) "K-7 Thermos, neutron thermalization in a heterogeneous cylindrically symmetric reactor cell", Kjeller Research Establishment, Kjeller, Norway.

Wagner R. (1970) Neutron wave experiments in a heavy natural uranium subcritical assembly. *J. nucl. Energy* **24**, 71.